Kinetics of Degradation of PVC-Containing Novel Neem Oil as Stabilizer

Padmasiri K. Gamage,[1] Ahmed S. Farid,[1] L. Karunanayake[2]

[1]*London Metropolitan Polymer Centre (Formerly The Open University of Sri Lanka), London Metropolitan University, London N7 8DB, United Kingdom*
[2]*Department of Chemistry, University of Sri Jayewardenepura, Nugegoda, Sri Lanka*

Received 27 May 2008; accepted 9 November 2008
DOI 10.1002/app.29686
Published online 13 February 2009 in Wiley InterScience (www.interscience.wiley.com).

ABSTRACT: The effectiveness of adding epoxidized neem oil (ENO) in poly(vinyl chloride) (PVC) to enhance heat stability was investigated. Neem oil, of vegetable extract, was characterized for its fatty acid profile and other properties. The virgin oil was epoxidized at 60°C with peroxymethanoic acid (performic acid) generated *in situ* in the reaction mixture by reacting hydrogen peroxide and methanoic acid. ENO was characterized by FTIR and NMR studies, and the degree of epoxidation was measured with iodine value and oxirane oxygen content. Solubility parameters of neem oil and ENO were estimated. Thermal degradation of PVC-containing ENO was studied using the static heat stability test and artificial aging at temperatures of 100, 110, 120, and 130°C. Results were compared with the samples prepared with conventional heat stabilizers systems used in PVC, such as Ca/Zn stearates and mixtures of both Ca/Zn stearates and ENO. The changes in elastic modulus of the ENO/PVC combination and the conventionally stabilized Ca/Zn system during aging were kinetically modeled, and the rate constants for the degradative influence of modulus were determined. The activation energies and preexponential factors for the degradative process were obtained from Arrhenius plots and their relationship through a compensation effect was found. In general, ENO was found to be an effective retarder of the degradation of PVC; use of 10 phr level of ENO showed the least degradation with the highest activation energy. A synergistic effect of ENO and Ca/Zn stearate system was also observed. © 2009 Wiley Periodicals, Inc. J Appl Polym Sci 112: 2151–2165, 2009

Key words: epoxidized neem oil; PVC; degradation; thermal stabilization; kinetic modeling

INTRODUCTION

Poly(vinyl chloride) (PVC) is a versatile material with an extensive range of applications. It is one of the three most abundantly produced polymers and one of the earliest that was developed.[1] An inherent disadvantage in the manufacture and use of PVC is its low thermal stability. For many applications, which require PVC, longevity is an important consideration and therefore its durability and stability needs to be authenticated. In this regard, heat stabilizers play an important role. The use of heat stabilizers in PVC compositions was first reported in 1930s.[2] Dehydrochlorination of PVC with elimination of hydrogen chloride (HCl) is generally believed to be the major cause of destabilization and degradation.[3,4] Dehydrochlorination also causes discoloration in the material. The color changes from white to yellow, brown, and finally to black. Change in color with the elimination of HCl is attributed to the formation of conjugated double bonds. Depending on the number of the conjugated double bonds formed, the color can range from yellow, orange, red, brown, or black.[5] Discoloration accompanies deterioration of some useful properties of the polymer; elastic modulus is one of the properties affected; it was observed that the elastic modulus increased because of the formation of crosslinks. The extent of crosslinking is a function of the swelling index or gel fraction; this was found to increase with increasing crosslink density.[6,7]

The main commercial heat stabilizers available for PVC are metal soaps, metal salts, and organometallic compounds. The mostly used metals from which these compounds are derived are lead, barium/zinc, calcium/zinc, and organotin compounds.[3] Epoxy compounds have also been identified as typical nonmetallic stabilizers for PVC. They are generally regarded as secondary stabilizers used to enhance the effectiveness of metal soaps. Epoxidized soybean oil is one such example of a nonmetallic stabilizer identified for its stabilizing action.[1,3,8,9]

Correspondence to: A. S. Farid (a.farid@londonmet.ac.uk).
Contract grant sponsor: National Science Foundation of Sri Lanka; contract grant number: RG/2006/FR/03.
Contract grant sponsor: Distance Education Modernisation Project of Asian Development Bank; contract grant number: 1999-SRI (SF).

Variety of vegetable oils whose physicochemical properties and fatty acid composition are similar to soybean oil are found in nature. The use of these natural oils in PVC formulations will address the crisis of fossil fuel depletion and the toxic effects of conventional plasticizers and stabilizers that are currently in use. In view of this, there are pressures imposed on researchers to work on these possible alternatives, which are derived from renewable raw materials that are nontoxic, under-exploited, and unutilized.

Stabilization effect of khaya seed oil, its epoxidized product, and metal soaps of khaya seed oil was reported by Okieimen et al.[10] These workers carried out degradation studies on PVC powder in the presence of khaya seed oil derivatives at various temperatures and determined the rate of dehydrochlorination titrimetrically. Furthermore, the same group of workers performed intrinsic viscosity and FTIR measurements on degraded PVC to assess the effectiveness of epoxidized khaya seed oil; they found that such oils can act as costabilizers in PVC formulations. A study of the use of epoxidized esters of palm olein as effective plasticizers suggested that the epoxidation of oil derivatives were essential as it improved compatibility as well as thermal stability.[11] Use of epoxidized sunflower oil on thermal degradation of PVC was investigated in the presence and absence of Ca/Zn and Ba/Cd stearates by Benaniba et al.[12,13] It was also reported that epoxidized rubber seed oil enhanced stabilization of PVC as well as acting as a secondary plasticizer.[14,15] A recent study on the use of epoxidized vegetable oils as thermal stabilizer for PVC conducted by Okieimen[16] has shed some light on the relative thermal stabilizing ability of epoxidized jartropha seed, khaya seed, and rubber seed oils; this work indicated that the metal soaps of these oils were found to be effective in retarding the rate of the dehydrochlorination of PVC and reducing the extent of chain scission reaction associated with the degradation of the polymer. A recent investigation on the effect of Zn soap of rubber seed oil and epoxidized rubber seed oil on the thermal stability of PVC plastigels has demonstrated some degree of synergism between the metal soaps and epoxidized rubber seed oil in terms of stabilization of PVC. Conductivity measurements have been reported for the kinetic characterization of dehydrochlorination of PVC plastigels; thus allowing the determination of relevant kinetic parameters such as activation energy and preexponential factor.[17]

Most of the aforementioned studies on dehydrochlorination and degradation of PVC were carried out in small laboratory-scale environments using solvent-cast films or by direct mixing of constituents in digestion tubes. Such methods avoided complications arising from bulk effects. In this work, we have utilized conventional fabrication techniques that are normally used in the polymer manufacturing industries; such techniques used will be described in the "Experimental" section. The preliminary literature search has indicated that there is a paucity of information concerning the way in which mechanical properties of PVC change with time and temperature. In view of this, the work described here studies the kinetics of degradation of PVC in terms of the elastic modulus. Moreover, a further novel aspect of this work is that we have introduced neem oil in our PVC polymer in addition to various other additives that are conventionally added to products made form PVC. Here, we consider it expedient to briefly describe the nature of neem oil.

Neem oil is a vegetable extract pressed from the fruits and seeds of neem (*Azadirachta indica*), an evergreen tree that is endemic to the Indian subcontinent. The whole parts of the neem tree (leaves bark and so on) are considered equally important in the field of indigenous medicine, covering a wide range of afflictions (skin diseases, inflammations, and fevers). Neem oil is used for preparing cosmetics such as soap, hair products, body hygiene creams, hand creams, and so forth. Formulations using neem oil is also found in a broad range of products such as biopesticides and insecticides.[18] In composition, it is much like other vegetable oils composed primarily of triglycerides of oleic, stearic, linoleic, and palmitic acids.

EXPERIMENTAL

Materials

Neem oil was obtained from D. Peiris, Colombo, Sri Lanka. Hydrogen peroxide was acquired from East Anglia Chemicals (40% w/v) and from Fisher Chemicals (UK) (30% w/v) and was standardized before use. Analytical reagent-grade formic acid obtained from Fisher Scientific (UK) was used after standardization.

The suspension homopolymer of PVC (ICI *K* value of 65, ISO viscosity 125) was acquired from European Vinyl Corporation, UK. The standard plasticizer, di(2-ethyl) hexyl phthalate (technical grade) was obtained from CIBA-Geigy (UK). Technical-grade calcium stearate and zinc stearates were purchased from Fisher Scientific. All other chemicals and solvents were classified as technical grades and used as received without further purification.

Epoxidation of neem oil

Epoxidation of neem oil was carried out at 60°C using performic acid prepared *in situ* by reacting hydrogen peroxide and formic acid. The molar ratio of mol of unsaturation : mol of formic acid: hydrogen

peroxide was kept as 2 : 1 : 4, respectively. The reaction was carried out on a relatively large scale using 1 kg of oil according to the following procedure: The required quantity of H_2O_2, equilibrated at 5–10°C, was added dropwise to a quantitative mixture of neem oil and formic acid into a 5-L flask. After adding all of the hydrogen peroxide, temperature of the reaction mixture was raised to 50–60°C and maintained within this range for 4 h with continuous stirring; at the end of this period, the entire mixture was added to a large vessel containing water and a given amount of solid $NaHCO_3$. The mixture was then rinsed with water until free from acid. Finally, the product was stirred with saturated sodium chloride solution, and then the top water-free layer of oil derivative was isolated.

Characterization of neem oil/epoxidized neem oil

Fatty acid profile of neem oil was obtained by using a Varian star 1 GC-MS instrument. For this purpose, oil was methylated according to the standard procedure using BF_3/methanol solution.[19] FTIR spectra of virgin oil and epoxidized oil were recorded by a Thermo Nicolet AVATAR 320 FTIR spectrometer coupled with Ezominic software; briefly, the principle of the procedure was to apply a thin layer of sample over a NaCl cell and record the spectrum in the range 400–4000 cm^{-1}. NMR spectra were recorded using BRUCKER AVANCE 500 NMR spectrophotometer. As regards with NMR experiments, frequencies of 500 MHz and 125.7 MHz were used for recording ^1H and ^{13}C spectra, respectively, and the solutions used were prepared in deuterochloroform using TMS as reference. Viscosity measurements were made using a Brookfield model RV-DVE 230 viscometer. Oxirane content and iodine value were determined according to the standard procedures.[19]

Preparation of test specimens

Samples were prepared using the following ingredients (parts by weight):

- PVC: 100 parts
- Di-2-ethylhexyl phthalate (DOP): 50 parts
- Stearic acid: 1 parts
- Ca/Zn stearates (1 : 1): 2 parts or/and
- Epoxidized neem oil (ENO): 5 or 10 parts

Batches based on 300 g of PVC were prepared. Ingredients were weighed to the nearest gram and hand mixed. The mixture was processed on a conventional laboratory-sized two-roll mill operating at 140°C until a coherent melt was obtained; the duration of this procedure was about 10 min. The fused PVC mixture was removed from the mill as a continuous sheet and subsequently compression-molded using a temperature and pressure of 150°C and 9266.5 kPa, respectively, to form sheets of dimension 152.4 mm × 152.4 mm × 1.14 mm.

TABLE I
Stabilizing Systems and Their Identification

PVC mix	Stabilizer system
0	Only Ca/Zn stearates (2 phr)
3.1	Only ENO (5 phr)
3.2	Only ENO (10 phr)
3.3	ENO (5 phr) + Ca/Zn stearates (2 phr)
3.4	ENO (10 phr) + Ca/Zn stearates (2 phr)

Five batches were prepared in the manner described earlier; each having a different stabilizer system. The stabilizers used and the labeling system used for their identification is delineated in Table I.

Static heat stability test

Circular test pieces (30-mm diameter) were punched from the previously prepared compression-molded sheets and placed in a circulating air oven maintained at 177°C ± 1°C and allowed to age. To monitor the required degree of aging, test pieces were removed at intervals of 5, 10, 15, 30, 45, 60, 75, 90, and 130 min.

The concomitant color changes with the aging process were observed using a Minolta spectrophotometer using the conditions specified below:

Settings: Condition 1
Mode ▶L UV ▶100%
Illuminant 1▶ D65
Observer ▶ 10^0 [Specular included (SCI)]

Tensile properties

A TINIUS OLSEN tensometer coupled with extensometer and QMat software was used for the determination of tensile properties. Standard dumpbell-shaped test pieces was punched (a standard cutter; ISO 37, type 2) using a single stroke of a hand press from the compression-molded sheets (prepared as in section "Preparation of test specimens"). The tensometer settings used for the determination of stress–strain properties were as follows:

Load range = 250 N
Extension range = 150 mm
Gauge length = 25 mm
Speed = 25 mm min^{-1}

Kinetic studies

Tensile dumbbells similar to those used for characterizing the tensile properties were utilized for studying kinetic behavior. In principle, as is

TABLE II
Comparative Compositions of Soybean and Neem Oil

Fatty acid	% Composition	
	Soybean oil [20]	Neem oil
Palmitic acid (16 : 0)	11	11
Stearic acid (18 : 0)	4	14
Oleic acid (18 : 1)	23	42
Linoleic acid (18 : 2)	53	32
Linolenic acid (18 : 3)	8	–
Total unsaturation	85%	74%

common with most kinetic studies, the procedure involved aging test pieces over a range of temperatures (100, 110, 120, and 130°C) and times. As before, a circulating air oven was utilized as the aging medium. The properties considered pertinent for kinetic characterization are as follows: elastic modulus, elongation at break, and the tensile strength. In particular, measurements of the elastic modulus were continued until a constant or steady-state value was attained.

The degree of volatility of DOP was ascertained by quantitative FTIR analysis using a common ratio method. In this method, peak heights were taken at two wave numbers (2920 and 1600 cm^{-1}) in the FTIR spectra obtained for sample 0, before aging and after 48 h aging at 130°C. The analysis ratio (L) was calculated using eq. (1):

$$L = \frac{\log\left(h_0 \Big/ h\right)_{v1}}{\log\left(h_0 \Big/ h\right)_{v2}} \quad (1)$$

where ($h_0 - h$) is the peak height at wave numbers 2920 cm^{-1} ($v1$) and 1600 cm^{-1} ($v2$), respectively.

Equilibrium swelling

Accurately weighed (m_1; 0.15 ± 0.2 g) specimens aged at 130°C for different periods of time were immersed in ~ 25 cm^3 of tetrahydrofuran maintained at 25°C ± 1°C in the dark until a state of equilibrium swelling was attained. The equilibrium mass of the specimens were accurately measured in a glass bottle with a ground stopper. The dried mass of the specimen (m_2) were then obtained after drying in a vacuum oven at 40°C, until constant weight was reached. Percentage gel fraction was calculated as $\{m_2/m_1\} \times 100$.

RESULTS AND DISCUSSION

Characterization of neem oil/epoxidized neem oil

Fatty acid composition of neem oil evaluated by its GC-MS is given in Table II and compared with the composition of soybean oil.[20] The use of soybean's expoxidized product in PVC formulations is extensively documented.[1,3,8,9,21] Other pertinent properties of the neem oil and ENO are delineated in Table III. Regarding these properties, percentage epoxidation of ENO was calculated based on the reduction of iodine value, before and after the epoxidation (The structure of a possible triglyceride and its epoxidized product is given in Fig. 1). The epoxidized product was characterized by FTIR and NMR studies, and the conversion of olifinic groups to epoxy groups was clearly indicated in spectra. Concerning the spectra, disappearance of the band 3010 cm^{-1} in FTIR indicates that C=C bonds has been consumed; a band around 820–830 cm^{-1}, which is not seen in pure oil, is characteristic to the epoxide and it was attributed to ring vibrations of the epoxy ring in cis epoxides.[22]

The proton NMR spectra of virgin oil and the epoxidized oil are shown in Figure 2.

The epoxy protons are observed at 2.8–3.0 ppm in the spectrum of epoxidized oil, whereas olifinic protons appeared in the region 5.2–5.4 ppm in spectrum of virgin oil. This peak is weakly observed because of the traces of unreacted groups remaining in the spectrum of epoxidized oil. Both peaks appeared as a quartet because of the coupling of two adjacent protons on the CH_2 group and the cis coupling of the proton attached to the subsequent sp^2-hybridized carbon atom. Terminal methyl groups are appeared as triplets in the range 0.7–1.0 ppm in all spectra.

The methine proton of the CH backbone of the glycerol carbon is observed at 5.1 ppm as a triplet in both cases, whereas the adjacent methine protons gives a characteristic double doublet pattern

TABLE III
Some Intrinsic Properties of Neem Oil (conventional and epoxidized)

Property	Neem oil	Epoxidized neem oil (ENO)
Appearance	Greenish brown liquid	Yellow liquid
Specific gravity	0.9259	0.9770
Refractive index	1.4745	–
Saponification value	177	–
Iodine value	109	07
Oxirane content	–	3.21
Viscosity (cP)	203 (21°C)	440 (50°C)
% epoxidation	–	94
Molar mass ($g\ mol^{-1}$)	314.4	330.4
Molar volume ($cm^3\ mol^{-1}$)	327.6	338.2
Solubility parameter (δ) ($cal\ cm^{-3})^{1/2}$	10.6	9.97
The χ value	0.7	0.257

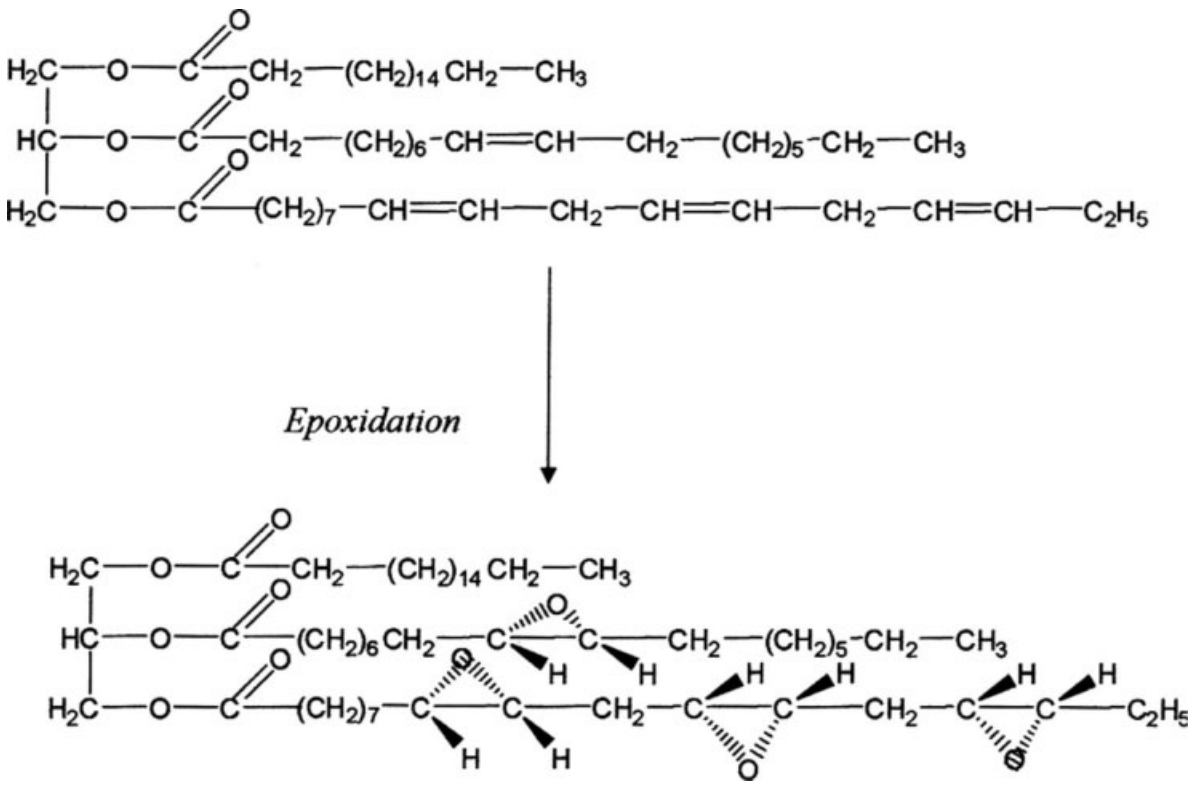

Figure 1 Structure of a possible triglyceride and its epoxidized product.

between 4.1–4.35 ppm, which is common for both epoxidized and virgin oils.

On the other hand, sp^2-hybridized carbon in olifinic groups appeared in the range 125–130 ppm in ^{13}C spectra of virgin oil, which are not observed in epoxidized oil (see Fig. 3), instead peaks appeared in the range 50–60 ppm indicating that epoxy carbon atoms appeared as CH.

Fatty acid profile of the neem oil and the general structure of a glyceride were taken into consideration when estimating molar masses of neem oil and ENO. Solubility parameters were calculated from the molar attraction constant values G, using Small's equation [eq. (2)]. The χ values were then subsequently determined using eq. (3). The thermodynamic concept for miscibility and the compatibility is that the smaller the difference between solubility parameters, the higher is the miscibility of the components. The δ values for PVC and DOP are 9.7 and 8.8, respectively. The δ value obtained for ENO is 9.97; this value is in good agreement with PVC/DOP combination.

$$\delta = \frac{d}{M}\Sigma G \tag{2}$$

$$\chi_1 = \chi_s + \frac{V_1(\delta_L - \delta_P)^2}{RT} \tag{3}$$

where d is the density; M is the molar mass of the substance; χ_s is an entropic term (usually assigned a value of 0.2); V_1 is the molar volume; δ_L and δ_P are the solubility parameters for the liquid and polymer, respectively; R is the gas constant and T is the absolute temperature.

Static heat stability test

It is understood that the degradation of PVC is initiated with dehydrochlorination, leading to the formation of a conjugated polyene structure (Fig. 4, reaction 1). The evolved HCl will accelerate the degradation process and, in this regard, the function of the heat stabilizer is to remove liberated HCl from the system to prevent an acceleration of the degradation process. Metal soaps such as zinc stearates remove HCl by reacting with it (see Fig. 4, reaction 2). Removal of tertiary or allylic chlorine atoms, which are largely responsible for the degradation of polymer chains, is also important in stabilizing mechanism. According to the Frye and Horst mechanism, these active Cl atoms are substituted by the carboxylate group of the metal soap and prevent initiation of dehydrochlorination.[5] The formation of $ZnCl_2$ (Lewis acid) due to reaction 2 also favors the dehydrochlorination step in reaction 1. Therefore a second metal soap, which will not form another Lewis acid and can convert the lewis acid produced from the first metal soap into its salt, is generally added. Calcium stearate couples with Zn stearate for

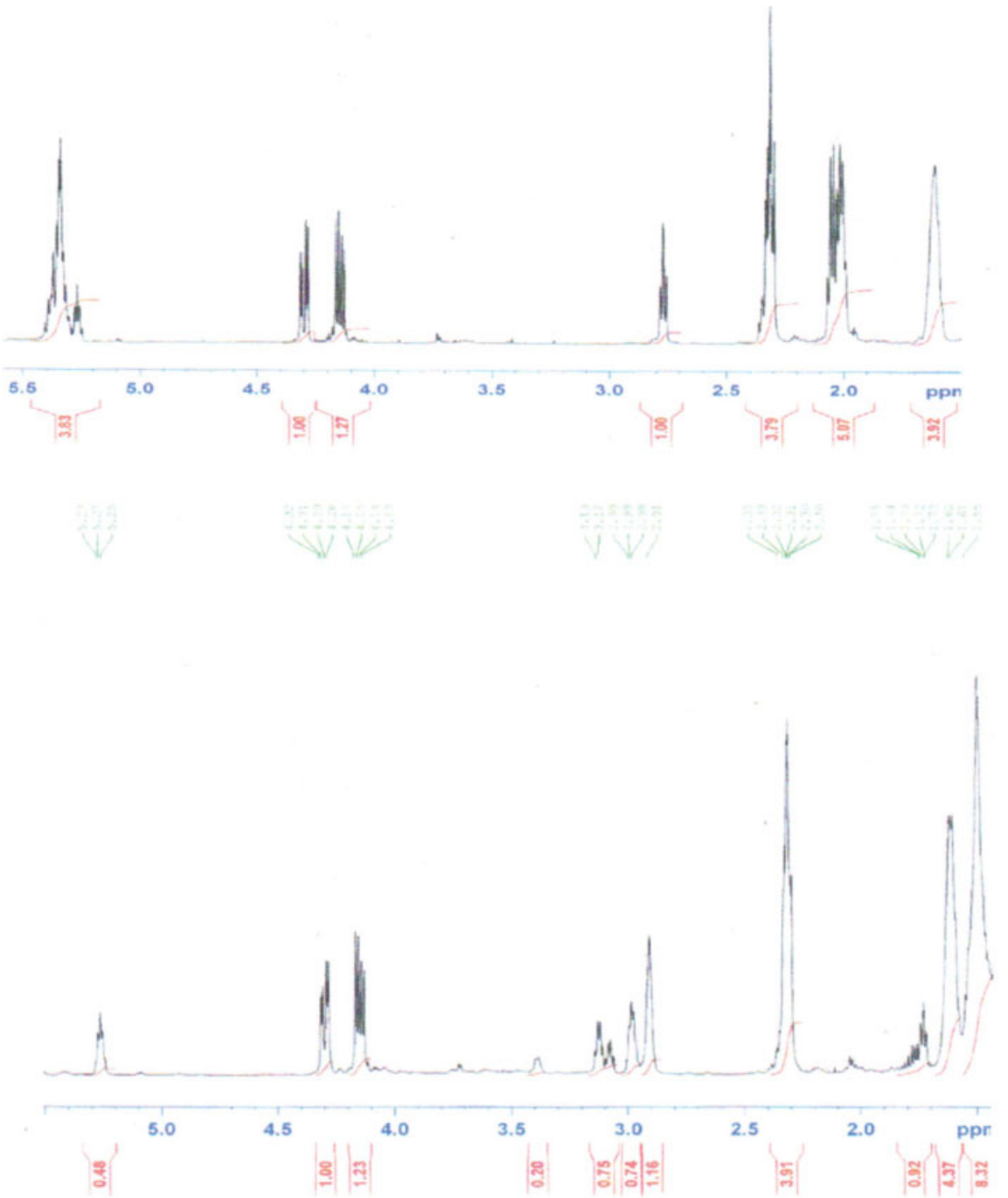

Figure 2 ^{1}H-NMR of neem oil (top) and epoxidized neem oil (bottom).

this purpose. Reaction 3 in Figure 4 shows the removal of HCl by epoxy groups in epoxidized oil derivative.

The neutralization effect of a stabilizer is primarily determined by its ability to prevent discoloration of PVC. In terms of discoloration, the illustrations in Figure 5 clearly show that the presence ENO has an inhibitive effect on thermal degradation of PVC. Moreover, the stabilizing effect of ENO is significantly greater when compared with the standard metal soap stabilizing system (Sample 0) notably a system based on Ca/Zn stearates. A synergistic effect is observed when both the metal soap system and the oil derivative are incorporated. Standard Ca/Zn stearate system is stable only up to 30 min; thereafter degradation occurred with celerity through dehydrochlorination resulting in the formation of a black brittle material at the latter stages of the degradation cycle. In passing, the reader should acknowledge that the color of the

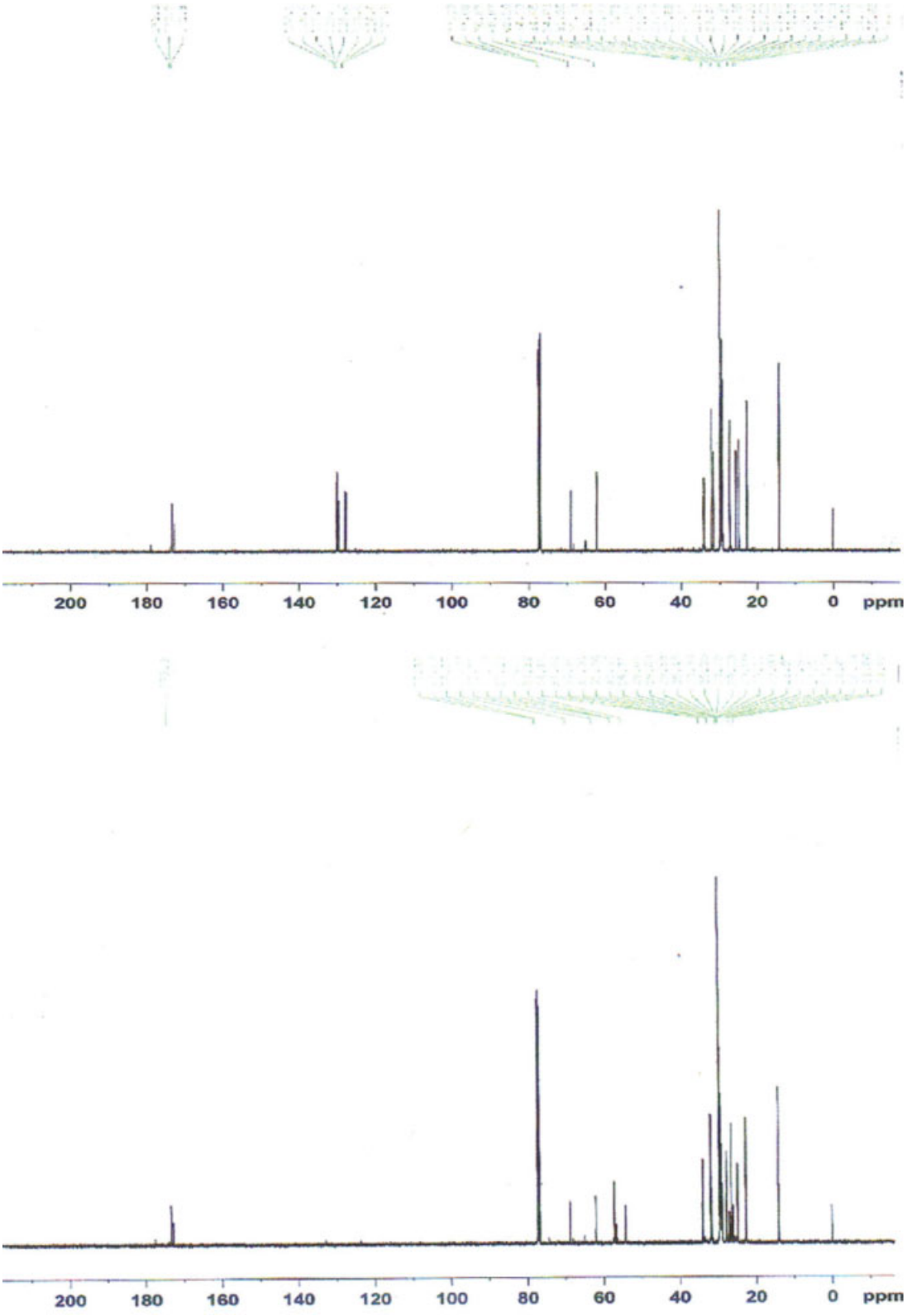

Figure 3 ^{13}C-NMR for neem oil (top) and epoxidized neem oil (bottom).

material changes from an innocuous condition (colorless appearance) to that which is black under severe degradation. The black color is due to the formation of conjugated polyenes and the concomitant hardening is due to extensive crosslinking between linear chains.[4]

When only oil derivative is incorporated as the stabilizer, the rate of degradation is reduced and

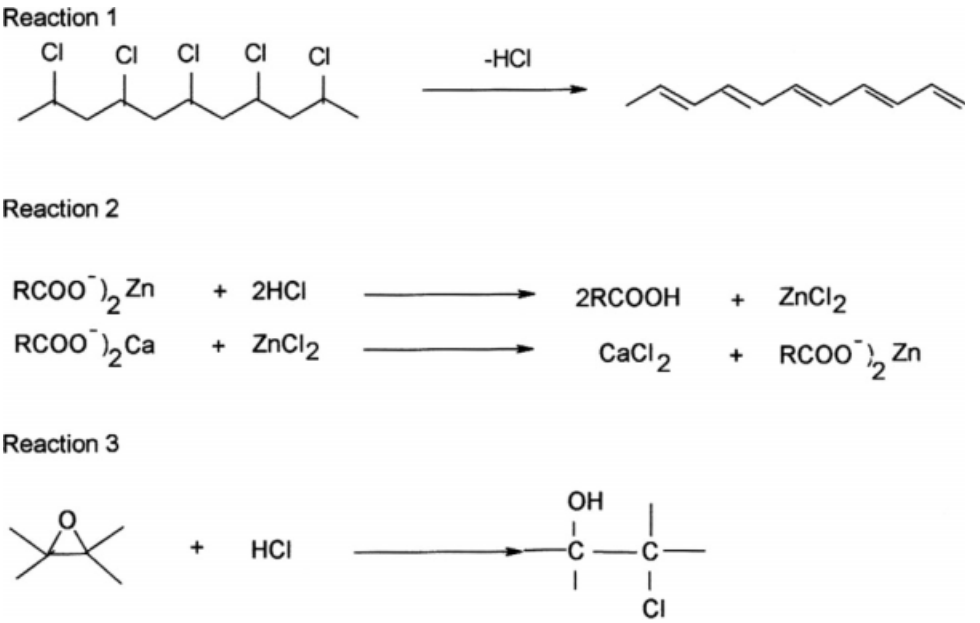

Figure 4 Reactions representing dehydrochlorination and removal of HCl.

there is no indication of surface blackening even after a period of 90 minutes. This observation suggests that the oil derivative increase the induction time of the degradation mechanism. The observed color of samples 3.1and 3.2 was pinkish brown to blood red. It was also found that increasing the level of oil derivative enhanced stability. Thus, a system comprising 10 phr level of ENO performed better than that containing 5 phr level. The severity of the dark color of samples 3.1 and 3.2 is mainly due to the color imparted by the oil derivative, which can be neutralized by using an appropriate color pigment. In general, it was found that the exudation of the oil derivative occurred when the concentration level exceeded 10 phr.

These results indicate that a combination of Zn/Ca metal soaps and epoxidized oil derivatives are effective in retarding the development of discoloration of PVC. Moreover, the epoxidized oil derivative is an effective stabilizer *per se* and does not need to depend upon synergism engendered by other additives. The system designated 3.4 contains Zn/Ca

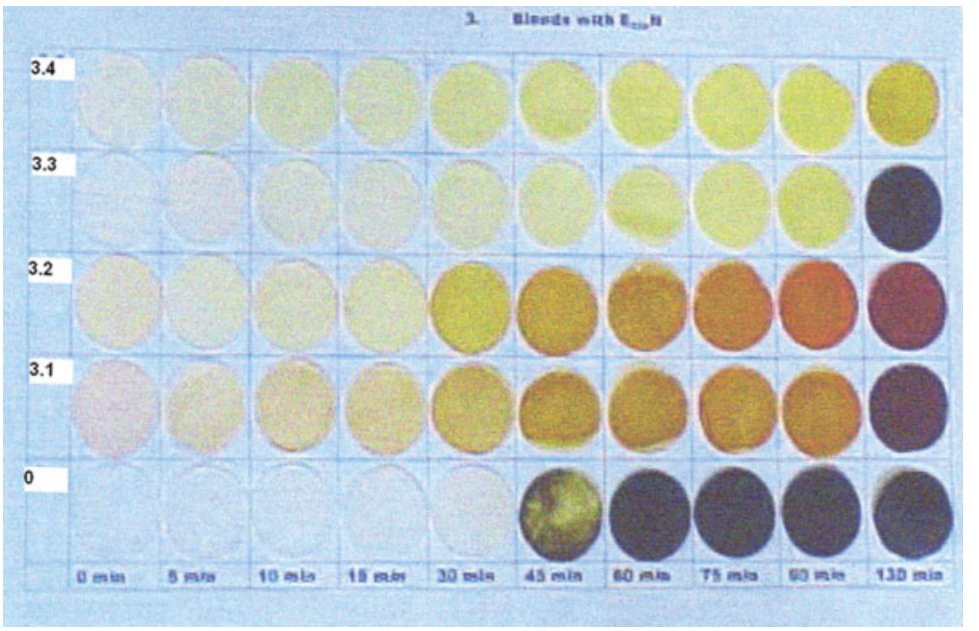

Figure 5 Variation of the color with time on aging at 177°C. [Color figure can be viewed in the online issue, which is available at www.interscience.wiley.com.]

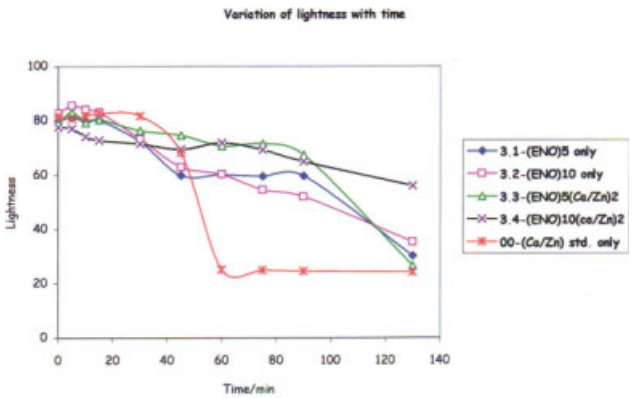

Figure 6 Variation of lightness with time on aging at 177°C. [Color figure can be viewed in the online issue, which is available at www.interscience.wiley.com.]

metal soaps combined with 10 phr level of ENO was found to be the most effective stabilizing system. The color variation of these samples may be described as off-white/light yellow to brown, which is significantly different from the remaining samples in the present series.

The synergistic effect of metal soaps–oil derivatives are ascribed by two reactions, notably esterification and etherification of allylic chlorine atoms as reported by Benaniba et al.[12] The combined effect of these two reactions would reduce the amounts of HCl evolved leading to the formation of short polyene sequences absorbing in the UV region. The color has been ascribed to the formation of polyene sequences of adequate size to allow absorption in the visible spectrum region. Essentially, metal soaps and epoxidized oil derivatives both act as HCl scavengers and thereby decelerate the degradation of PVC.

These results are further confirmed by the variation of lightness with time. According to Figure 6, the rate of decoloration is minimum in the sample designated 3.4. Color observations conclude that the chlorohydrin derivative formed by epoxidized oil derivative or the degraded product is red.

Tensile measurements

Elastic modulus, tensile strength, and percentage elongation at break were measured before and after aging at temperatures of 100, 110, 120, and 130°C (see Table IV). Aging at each temperature was continued until the elastic modulus had reached a steady-state value.

Comparison of the tensile properties of unaged samples showed that the system containing only 10 phr level of ENO (3.2) gave the lowest elastic modulus, the highest tensile strength, and the highest percentage elongation at break. This observation suggests that the material is softer and tougher when compared with others in the series. The lowest tensile strength and the lowest percentage elongation at break were shown by the sample comprising the standard Ca/Zn stabilizer system (0). Clearly, the tensile strength and the percentage elongation were enhanced with the addition of ENO. This alludes to the possibility of ENO acting as a plasticizer. Tensile properties of aged samples and their concomitant color variation with aging (see Fig. 7) showed the following characteristics.

Sample prepared with only Ca/Zn stabilizer (0) became harder, stronger, and embrittled at a significantly faster rate than the remaining samples. Moreover, Sample 0 was found to blacken within a relatively short period of aging. The trend in discoloration was slower in all other samples. The preceding results lead to the conclusion that the breakage of the long polymer chains (chain scission) leading to shorter chains reduces the percentage elongation at break. Formation of crosslinks among chains makes the material hard and hence a higher elastic modulus is observed. This was further ascertained by the increase in percentage gel fraction with aging time. Calculated percentage gel fractions for Sample 0, aged at 130°C after 24 and 48 h aging were 67 and 81%, respectively; zero gel fractions were obtained for samples aged below 24 h. The process was decelerated by ENO, which is incorporated as a stabilizer in all the other samples. The least degradation was observed in sample 3.2, that is, the sample containing 10 phr level of ENO, as stabilizer. The percentage gel fractions were found to be zero for sample 3.2 even after 48 h aging at 130°C. Thus, it appears that ENO is more effective when compared with the Ca/Zn stearates system in retarding the dehydrochlorination of PVC. However, the lower level of ENO (5 phr) is not adequate as it is consumed rapidly and consequently degradation occurs with impunity. The combined effect of ENO and Ca/Zn system seems to be effective over a limited period of time, as illustrated by the tensile data, force extension variation, and the color variation; at higher temperatures, however, poor performance was observed over extensive aging times. The foregoing observations are consistent with the decreasing percentage elongations to break. Therefore, it may be educed that the reaction between the Lewis acid, $ZnCl_2$, with the epoxy ring of ENO is preventing the reaction with HCl leading to rapid chain scission. The percentage elongation at break of the samples, after aging for 24 h at each specific temperature, showed no appreciable change from the original values (see Fig. 8); however, the elastic modulus was increased significantly. After extensive aging, the percentage elongation at break was decreased considerably in Sample 0. In other samples, however, the rate at which elongation at break decreased was slower when compared with Sample 0 (see Fig. 9).

TABLE IV
Variation of Tensile Properties with Time at Different Temperatures

Aging time (hours)	Elastic modulus (MPa)					Tensile strength (MPa)					% Elongation at break				
	00	3.1	3.2	3.3	3.4	00	3.1	3.2	3.3	3.4	00	3.1	3.2	3.3	3.4
Aging at 100°C															
0	5.8	6.3	4.9	6.3	5.9	12.5	14.1	14.8	14.6	14.4	240	262	332	251	278
7	52	11.7	10.8	12	10.7	16.0	15.6	14.1	15.8	15.3	172	172	168	170	187
24	169	150	122	195	152	20.1	22.6	20.0	20.5	20.8	153	204	197	171	198
48	502	305	199	414	300	25.7	25.4	21.5	25.3	22.7	175	189	198	205	205
72	519	400	257	420	551	26.3	26.6	23.6	24.3	21.0	193	192	188	185	169
144	700	810	688	756	681	29.9	30.1	27.8	28.4	24.3	151	186	181	189	174
192	674	945	651	840	721	29.9	31.1	28.6	25.6	25.6	173	183	163	162	193
240	699	951	599	888	695	31.5	35.0	27.0	28.7	30.2	139	114	187	174	156
312	712	967	857	863	1088	35.6	37.2	33.7	36.2	34.5	80	182	77	148	174
360	778	803	807	920	899	35.0	32.0	34.0	33.0	31.0	51	147	48	152	123
480	888	980	812	821	1002	42.0	43.0	41.0	37.0	36.7	58	47	52	153	161
528	822	833	873	814	911	41.0	39.0	34.0	34.0	36.0	57	73	140	105	107
Aging at 110°C															
2	8	9	8.5	9	8.3	18.2	18.9	18	18.4	17.0	217	225	234	228	226
4	117	69	58	83	66	18.9	18.2	17	19.3	16.0	214	211	212	205	177
7	190	110	120	120	100	20.3	20.1	18.5	19.2	20.0	185	201	198	188	222
24	454	249	240	367	350	25.1	23.9	23	23.3	23.2	201	185	217	180	217
31	899	466	403	622	429	28.0	28.2	24.9	25.9	25.1	191	215	190	191	220
48	959	695	620	710	848	27.7	27.2	26.7	25.9	26.5	175	191	212	185	212
72	913	784	439	978	1007	31.8	28.7	26.7	29.1	27.7	166	175	196	192	210
96	850	591	606	1056	956	31.1	30.9	26.8	29.5	26.5	130	110	186	172	195
168	976	588	617	971	1208	38.8	40.5	31.6	35.2	30.5	68	75	188	189	179
240	1074	740	636	1128	1126	49.8	48.0	40.2	46.1	40.8	09	57	149	42	40
336	1054	926	737	1141	990	51.5	47.3	37.8	46.7	41.0	20	89	178	37	44
Aging at 120°C															
1.5	78	7.5	4.3	39	7.6	17.5	17.2	16.7	17.9	15.4	196	226	235	220	179
3	123	55	33	110	45	20.2	15.1	15.7	19.3	18.7	214	207	198	207	236
5	161	80	49	128	71	18.8	19.4	17.1	19.9	19.4	175	206	203	204	207
7	305	115	77	144	149	21.4	19.7	18.1	21.4	18.3	179	201	194	207	210
24	741	407	229	630	497	26.8	25.3	22.9	25.7	22.6	188	178	190	197	186
31	833	526	270	617	540	30.7	27.9	26	26.5	25.3	160	196	191	173	199
48	693	670	400	685	680	29.8	28.8	25.7	27.7	27.6	136	179	170	168	194
72	953	707	556	726	813	36.1	32.3	29.2	31.8	32.1	117	173	188	152	145
144	1056	928	746	945	1054	46.4	50.1	39.7	45.3	39.9	19	114	157	47	18
192	1001	1069	812	1248	1138	54	42.7	37.9	47.5	41.5	17	71	103	27	25
240	1183	1153	1049	1218	1148	53.4	54.2	48.1	52.5	46.3	18	45	42	14	16
Aging at 130°C															
1	8	8	8.4	9	8.7	17.4	18.2	16.1	17.0	16.4	194	224	209	206	210
4	200	114	77	152	153	20.5	20.2	20.1	20.0	19.3	171	195	218	171	201
7	526	314	200	311	240	23.0	23.0	21.7	20.0	21.9	144	189	203	151	217
24	714	606	441	758	647	30.0	25.6	23.8	26.9	24.2	59	162	166	143	167
31	875	667	9694	883	953	41.0	36.0	30.6	37.0	31.8	10	169	188	149	135
48	896	842	744	1028	925	42.4	38.5	31.4	39.7	32.7	22	114	160	81	133
55	1237	1029	779	1034	984	49.0	42.0	37.7	43.0	38.0	12	35	53	36	41
72	1143	868	941	1047	1023	46.0	40.7	38.2	42.0	41.0	17	61	151	32	17
96	1154	949	1108	1075	1399	49.0	42.8	41.2	43.0	42.7	08	39	46	10	14

Kinetic modeling

By using simple mathematical transforms, it was found that a significant relationship could be obtained between the logarithm of the modulus (log E) and aging time. Such relationships found are illustrated in Figure 10. The form of the relationship shown in Figure 10 suggests direct proportionality between the slope at any point on the curve and the difference between the asymptotic value of log E (log E_∞) and the log E value at the point at which the slope is taken.

That is, $\frac{d}{dt}(\log E) \propto (\log E_\infty - \log E)$; therefore, by introducing a constant we obtain

$$\frac{d}{dt}(\log E) = -k(\log E_\infty - \log E) \quad (4)$$

where E = E-modulus; E_∞= E-modulus at steady state; k = proportionality constant that can be considered as the rate constant.

Figure 7 Variation of color with aging time at different temperatures. [Color figure can be viewed in the online issue, which is available at www.interscience.wiley.com.]

Rearrangement of eq. (4) gives

$$\frac{d \log E}{\log E_\infty - \log E} = kdt$$

Integration of the above expression leads to

$$\ln(\log E_\infty - \log E) = -kt + c \qquad (5)$$

In eq. (5), c is the constant of integration. The form of eq. (5) indicates that a plot of $\ln(\log E_\infty - \log E)$ against aging time (t) should be linear with gradient k, which is the rate constant of the degradation process.

The plots of $\ln(\log E_\infty - \log E)$ against aging time (t) at different temperatures for the complete series of samples investigated are given in Figure 11. $\log E$ values were obtained the best fits of the plots of $\log E$ vs. time. The $\log E_\infty$ values are also extrapolated from the curves. All plots showed excellent agreement with eq. (5). The linear equations thus obtained together with their R^2 values are given in Table V.

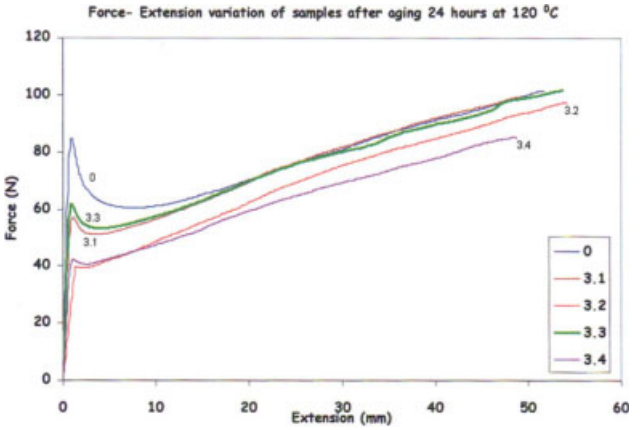

Figure 8 Force-extension variation after 24 h aging at 120°C. [Color figure can be viewed in the online issue, which is available at www.interscience.wiley.com.]

However, the elastic modulus on aging can increase because of the evaporation of DOP from PVC. The quantitative FTIR analysis on Sample 0, before aging and after 48 h aging at the highest temperature used in the study (that is 130°C) confirms that the volatility loss of DOP is negligible under the temperature range used in this study. The peak heights at 1600 cm^{-1}, which is characteristic to phenyl rings were compared with reference. Calculated values for L using eq. (1), before and after aging were 10.3 and 10.7; these values are clearly almost identical.

The temperature dependency of the rate constant is given by the Arrhenius equation:

$$\ln k = -\frac{E_a}{R}\left(\frac{1}{T}\right) + \ln A \qquad (6)$$

where k is the rate constant, T is the absolute temperature, A is the preexponential factor, R is the universal gas constant, and E_a is the activation energy.

The Arrhenius plots constructed with appropriate rate constants are given in Figure 12. Activation energies and preexponential factors were calculated from the gradient and the intercept, respectively; values obtained for activation energies are depicted in Figure 13. The equations representing the Arrhenius relationship, the calculated activation energies, and preexponential factors are given in Table VI.

The activation energy of a chemical reaction reflects the kinetic stability of any system. Higher the activation energy, reactants are more kinetically stable and hence the reaction may not take place or take place at a slower rate. In the thermal degradation of PVC, HCl gas is evolved and the product is a solid residue. Hence, the reaction is heterogeneous. It is expected that the addition of a heat stabilizer to PVC should result in higher values of activation energy for dehydrochlorination, and the more effective the heat stabilizer system, the higher is the values of activation energy. Arkis et al. [23] reported that the activation energy for the dehydrochlorination of PVC in the presence of organotin heat stabilizers were in the range of 58–77 kJ mol^{-1} in the temperature range 140–180°C using thermogravimetry.

In this work, the highest activation energy obtained was 83 kJ mol^{-1} when 10 phr level of ENO was used as the heat stabilizer. Therefore, ENO, at a level of 10 phr level, is the most effective stabilizer system among the other stabilizer systems used in this study. The activation energy obtained for the standard Ca/Zn system was 74 kJ mol^{-1}, which is less than that of the system containing 10 phr of ENO. However, these calculations were based on the assumption that the activation energy does not change within the temperature range considered here (100–130°C).

Apart from the activation energy, the preexponential factor (A) is also important to describe the complex process of polymer degradation. From the data in Table VI, it is evident that the preexponential factors vary with the activation energies that could be as a result of reactions with dissimilar mechanisms. When log A and E_a exhibit a linear relationship for a

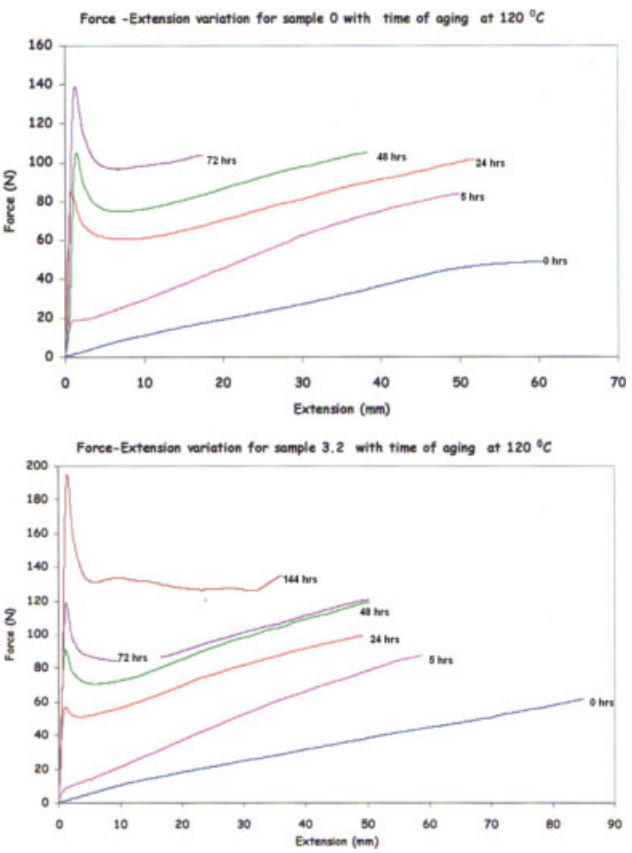

Figure 9 Force-extension variation for sample 0 (top) and sample 3.2 (bottom) with time (aging at 120°C). [Color figure can be viewed in the online issue, which is available at www.interscience.wiley.com.]

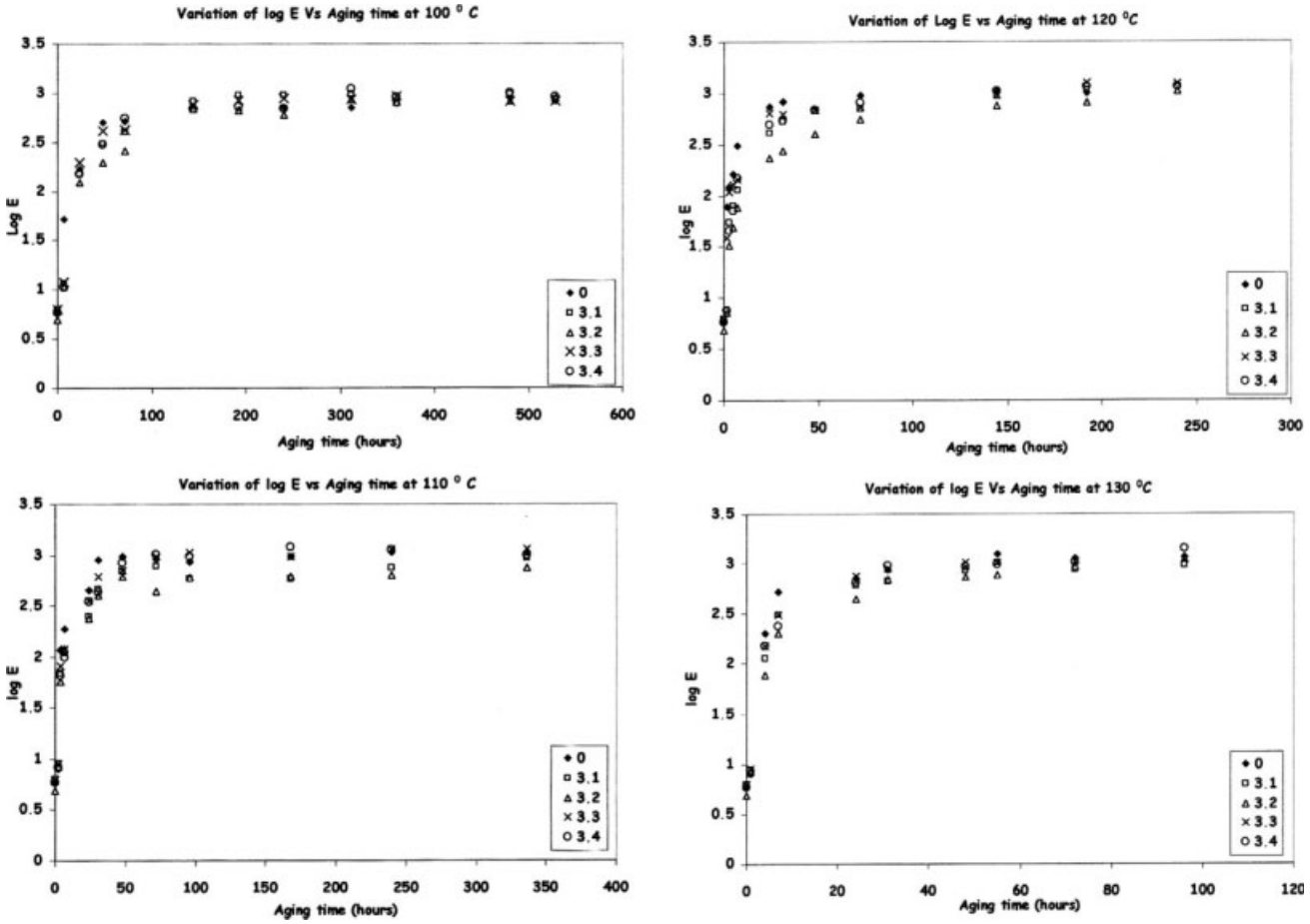

Figure 10 Variation of logarithm of elastic modulus (log E) with aging time at temperatures 100, 110, 120, and 130°C.

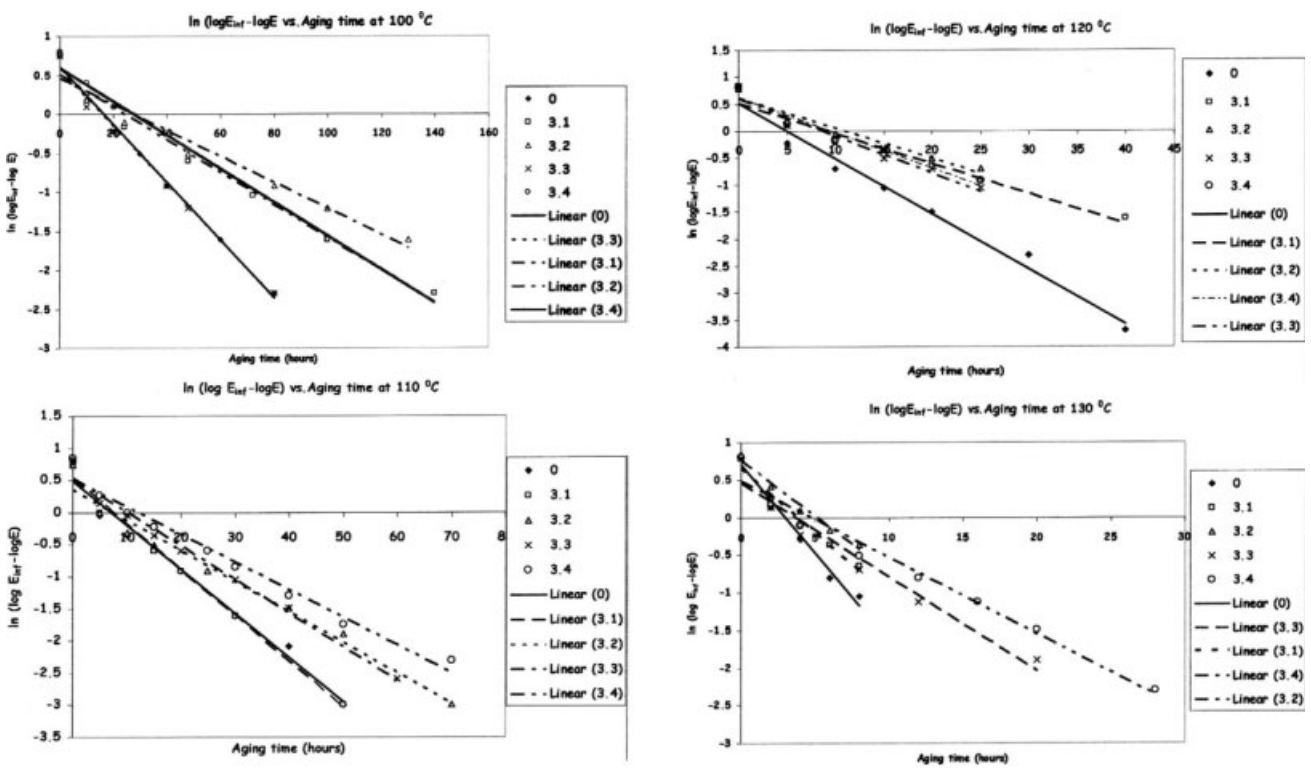

Figure 11 Straight-line plots obtained for the eq. (4) at different temperatures.

TABLE V
Linear Relationships and Rate Constants for Samples at Different Temperatures

Temperature (°C)	Sample	Equation $\ln(\log E_\infty - \log E) = -kt + c$	R^2 value	Gradient (k) = Rate constant (h^{-1})
100	00	$Y = -0.0371x + 0.6121$	0.9941	0.0371
	3.1	$Y = -0.0208x + 0.5018$	0.982	0.0208
	3.2	$Y = -0.0167x + 0.4542$	0.9545	0.0167
	3.3	$Y = -0.0366x + 0.5747$	0.9915	0.0366
	3.4	$Y = -0.0216x + 0.6109$	0.9879	0.0216
110	00	$Y = -0.0688x + 0.4937$	0.98	0.0688
	3.1	$Y = -0.0714x + 0.532$	0.9905	0.0714
	3.2	$Y = -0.0475x + 0.3542$	0.9736	0.0475
	3.3	$Y = -0.0525x + 0.533$	0.9845	0.0525
	3.4	$Y = -0.0432x + 0.5212$	0.9763	0.0432
120	00	$Y = -0.1024x + 0.52$	0.9805	0.1024
	3.1	$Y = -0.0566x + 0.5089$	0.9619	0.0556
	3.2	$Y = -0.0553x + 0.6078$	0.9464	0.0553
	3.3	$Y = -0.069 + 0.0604$	0.947	0.069
	3.4	$Y = -0.0657x + 0.6131$	0.9433	0.0657
130	00	$Y = -0.2348x + 0.7055$	0.9772	0.2348
	3.1	$Y = -0.1703x + 0.6541$	0.9621	0.1703
	3.2	$Y = -0.1478x + 0.7549$	0.9773	0.1478
	3.3	$Y = -0.1254x + 0.4598$	0.9564	0.1254
	3.4	$Y = -0.1016x + 0.4842$	0.9742	0.1016

series of related heterogeneous reactions, it is known as kinetic compensation effect or isokinetic effect.[24,25,26] The activation energy and preexponential factor are often connected by compensation relation as given in the eq. (7).[25]

$$\ln A = \frac{E_a}{RT_{\text{iso}}} + \ln k_{\text{iso}} \tag{7}$$

where k_{iso} and T_{iso} are the isokinetic rate constant and the isokinetic temperature. On the other hand, if a linear relation exists between ln A and E_a, it implies that the reaction follows the same mechanism, while any deviation from the straight line indicates different mechanism. In Figure 14, the dependence of ln A vs. E_a is shown and that shows the excellent linear relation that can be fitted to the eq. (8) with the correlation coefficient (R^2) 0.9975.

$$\ln A = 0.305E_a - 2.3788 \tag{8}$$

The compensation ratio; $E_a/\ln A$ can be used to describe the reactive ability of the system. The isokinetic temperature, the temperature at which the rate constants of all reactions of the series have the same value, was calculated from the gradient of the eq. (7) and found to be 394 K (121°C). The calculated isokinetic rate constant from the intercept was 0.093 h^{-1}.

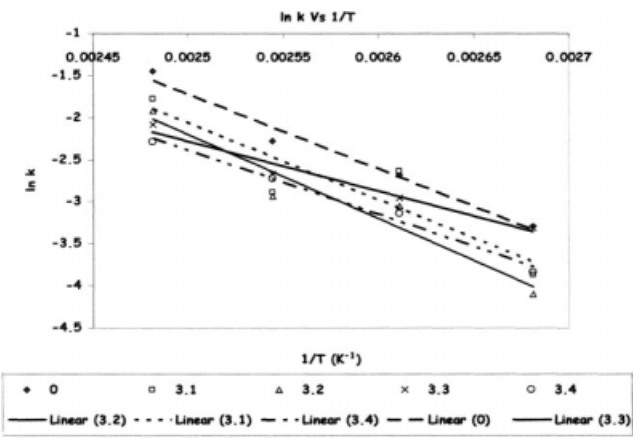

Figure 12 Arrhenius plots.

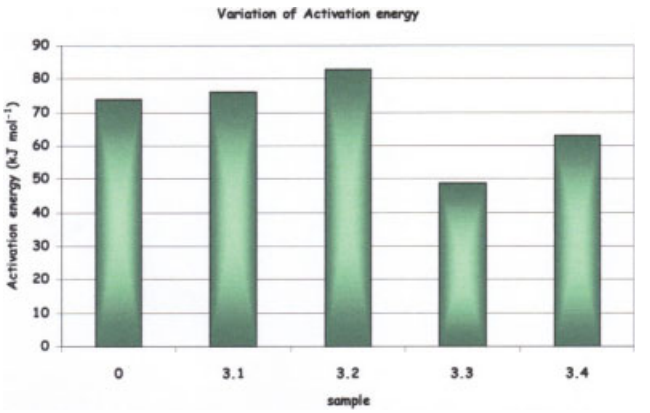

Figure 13 Variation of activation energies. [Color figure can be viewed in the online issue, which is available at www.interscience.wiley.com.]

TABLE VI
Linear Relationship to Arrhenius Plots, Calculated Activation Energies, and Preexponential Factors

Sample	Equation	R^2 value	E_a (kJ mol^{-1})	Preexponential factor (h^{-1})
0	$Y = -8898.9x + 20.53$	0.9778	74	8.2×10^8
3.1	$Y = -9112.8x + 20.713$	0.8187	76	9.9×10^8
3.2	$Y = -10005x + 22.812$	0.9294	83	8.1×10^9
3.3	$Y = -5943.7x + 12.58$	0.9658	49	2.9×10^5
3.4	$Y = -7629.7x + 16.684$	0.9887	63	1.8×10^7

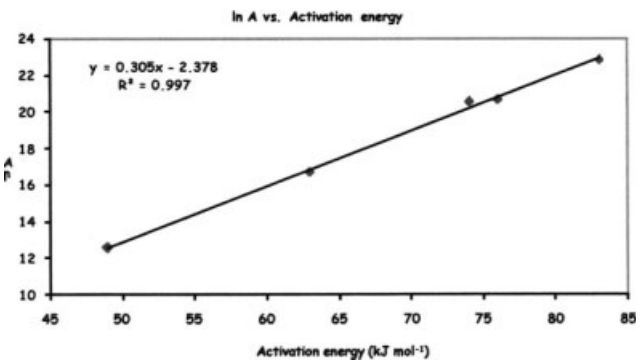

Figure 14 ln A vs. E_a for the degradation process of PVC stabilized with different stabilizer systems used.

CONCLUSION

This study was concerned with investigating the effectiveness of epoxidized neem oil (ENO) as a heat stabilizer in PVC. The stability provided by ENO in terms of changes in elastic moduli during high-temperature aging was modeled kinetically. It was found that the kinetic model obeyed a law of the form $\ln(\log E_\infty - \log E) = kt + C$. Activation energy values for the change in elastic modulus of PVC suggest that 10 phr of ENO is capable of retarding the degradation of PVC. The highest activation energy obtained for the ENO/PVC system was 83 kJ mol^{-1}. The activation energy and preexponential factor are linked by compensation relation describing the reaction ability of the system. The calculated solubility parameter (δ) value for ENO is 9.97. Epoxidized neem oil shows excellent properties as a stabilizer for PVC in the absence of any other metal soaps and it is found to be more effective than the standard stabilizer, for instance, the Ca/Zn stearates system. A synergistic effect is also observed when ENO is used in combination with Ca/Zn metal soaps.

Padmasiri is grateful to the Open University of Sri Lanka for the study leave, and the University of Sri Jayawardhenepura, Sri Lanka, for the initial assistance provided for this work.

References

1. Carraher, C. E., Jr. Seymour/Carraher's Polymer Chemistry; Marcel Decker: New York, 2003.
2. Titow, W. V. PVC Plastics-Properties Processing and Applications; Elsevier Science Publishers: London and New York, 1990.
3. Mathews, G. PVC- Production Properties and Uses; The Institute of Materials: Cambridge, 1996.
4. Penn, W. S. PVC Technology, 3rd ed.; London Applied Science: UK, 1971.
5. Gokcel, H. I.; Blakose, D.; Kokturk, U. Eur Polym J 1999, 35, 1501.
6. Sophie, G.; Emmanuel, B.; Jocelyne, G.; Jean Francois, G.; Michel, L. Polymer 2004, 45, 7739.
7. Karam, H. J.; Tien, L. J Appl Polym Sci 2003, 30, 1969.
8. Gachter, R.; Muller, H., Eds. Plastic Additives Handbook; Hanser Publishers: New York, 1996.
9. Ishiaku, U. S.; Shaharum, A.; Ismail, H.; Mohd. Ishak, Z. A. Polym Int 1997, 45, 83.
10. Okieimen, F. E.; Eromonsele, O. C. Eur Polym J 2000, 36, 525.
11. Gan, L. H.; Oii, K. S.; Goh, S. H.; Gan, L. M.; Leong, Y. C. Eur Polym J 1995, 31, 719.
12. Benaniba, M. T.; Belhaneche-Bensmera, N.; Gelbard, G. Polym Degrad Stab 2001, 74, 501.
13. Benaniba, M. T.; Belhaneche-Bensmera, N.; Gelbard, G. Polym Degrad Stab 2003, 82, 245.
14. Joseph, R.; Madhusoodhanam, K. N.; Alex, R.; Varghese, S.; George, K. E.; Kuriakose, B. Plast Rubber Compos 2004, 33, 217.
15. Okieimen, F. E.; Justus, E. J Appl Polym Sci 1993, 48, 1853.
16. Okieimen, F. E. Indus Crops Prod 2002, 15, 71.
17. Egbuchunam, T. O.; Balkose, D.; Okieimen, F. E. Polym Degrad Stab 2007, 92, 1572.
18. The Free Encyclopedia. Available at: http://neem oil-wikipedia.
19. Paquot, C., Ed. Standard Methods for the Analysis of Oils, Fats and Derivatives, 6th ed.; Pergamon Press: France.
20. Gunstone, F. D. The Chemistry of Oils and Fats: Sources, Composition, Properties and Uses; Blackwell: UK, 2004.
21. Baltaciodlu, H.; Balköse, D. J Appl Polym Sci 1999, 74, 2488.
22. Bellamy, L. J. The Infrared Spectra of Complex Molecules, 3rd ed.; Vol. 1, 1975.
23. Arkis, E.; Balkose, D. Polym Degrad Stab 2005, 88, 46.
24. Branka, A.; Tonka, K.; Ivka, K. Polym Degrad Stab 2003, 79, 265.
25. Natasa, S. V.; Ivka, K.; Tonka, K. Polym Degrad Stab 2004, 84, 31.
26. Stipanelov Vrandecic, N.; Klaric, I.; Roje, U. Polym Degrad Stab 2001, 74, 203.